Electromechanical Characterisation and Computer Simulation of a Noradrenaline Induced Ventricular Arrhythmia

Martyn Nash, Judith Thornton, Tony Varghese and David Paterson

University Laboratory of Physiology, Parks Road, Oxford OX1 3PT, U.K.

Supported by the British Heart Foundation *and* The Wellcome Trust

Introduction

It is well established that cardiac sympathetic imbalance can lead to ventricular arrhythmias, although the underlying cellular electrophysiological mechanisms are not fully understood. Abnormal automaticity and triggered activity have been implicated, since both can be provoked by catecholamines or exercise (Lerman *et al.*, *Circulation* **87**:382-390, 1993) and prevented or terminated by β-adrenergic blockade, calcium channel antagonists and acetylcholine (Wit *et al.*, *Circ Res* **41**:434-445, 1977), all of which modulate the levels of intracellular calcium in ventricular myocytes.

We induced a sustained ventricular arrhythmia in the *in-vivo* non-ischemic pig heart using a localised subepicardial infusion of noradrenaline (NA) as previously described (Podzuweit, *Basic Res Cardiol* **75**:772-779, 1980) . Our aim was to characterise the ventricular epicardial activation sequence in 3D during this arrhythmia to test whether local adrenergic imbalance caused an abnormal electrical activation pattern due to the formation of a new pacemaker at the infusion site. To elucidate the electrophysiological basis underlying this arrhythmia, we attempted to reconstruct it in 2D using a network model of 256 by 256 resistively coupled ventricular cells, for which the central region had high adrenergic tone.

Methods

- 14 domestic pigs (25±3 kg) were anaesthetised with α-chloralose (100 mg/kg i.v.), ventilated, thoracotomised and vagotomised.
- maintained core temperature (37±1 °C), fluid balance (*ca.* 100 ml/hr saline infusion) and arterial blood gases (PCO_2: 43±6 mmHg; PO_2: 298±81 mmHg; pH: 7.40±0.07).
- monitored ECG, arterial blood pressure (ABP), heart rate (HR), left ventricular pressure (LVP) and its rate of change (LVdP/dt).
- provoked ventricular arrhythmias by subepicardial infusion of NA (10μM in 0.9% saline, 150μl/min).
- recorded ventricular epicardial electropotentials using an elasticated electrode sock (inter-electrode spacing *ca.* 15 mm) connected to a 64 channel Unemap system (sampling rate 900 Hz).
- detected right atrial activation (n=10) using a single custom-built electrode.
- paced hearts (n=3) using a custom built roving bipolar electrode (0.5-1.5 V, 2 ms width, 30 s duration, n=3). The pacing rate was matched to the HR observed during the previous arrhythmia.

3D epicardial mapping

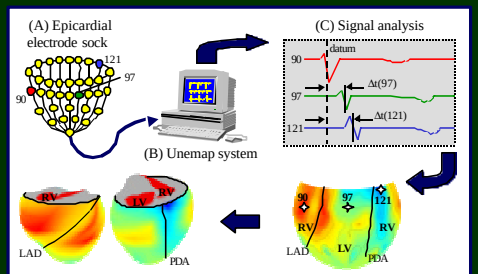

Figure 1. **(A)** Epicardial signals were recorded using an elasticated sock with 63 epicardial electrodes connected to **(B)** a Unemap cardiac mapping system. **(C)** A single heart cycle was identified and the epicardial activation time for each electrode was determined using the most negative electropotential slope. **(D)** An epicardial activation map was fitted to the electrode activation times and displayed using the Hammer projection. This 2D topography represents the ventricular epicardial surface, where the left ventricle (LV) makes up the central portion of the projection, the right ventricle (RV) comprises the border regions, but the apex is retained as a single point. **(E)** The activation time field was also fitted to the epicardial surface of a 3D anatomically accurate mathematical model of the ventricles, for which anterior and posterior views are illustrated. The left anterior (LAD) and posterior descending (PDA) coronary arteries have been superimposed for anatomical clarity.

Results

2D ventricular epicardial activation sequence

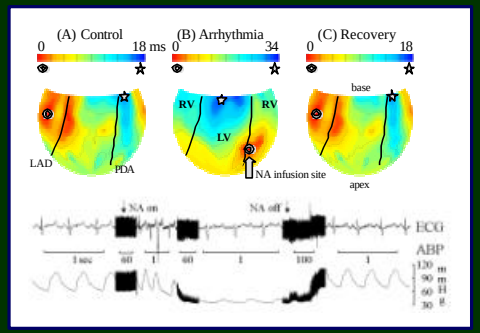

Figure 2. 2D epicardial activation sequences and cardiac function for one experiment during **(A)** normal sinus rhythm, **(B)** ventricular arrhythmia and **(C)** recovery, displayed using the Hammer projection. Isochronal contours (thin lines) separate regions of earliest (o) and latest (*) epicardial activation. Thick lines represent the left anterior descending (LAD) and posterior descending (PDA) coronary arteries. During the ventricular arrhythmia (panel B), the location of earliest epicardial activation shifted to the NA infusion site (thick arrow) and the QRS complex of the ECG inverted. Immediately following this event, the ABP dramatically decreased. After the infusion was stopped (panel C), the haemodynamics fully recovered.

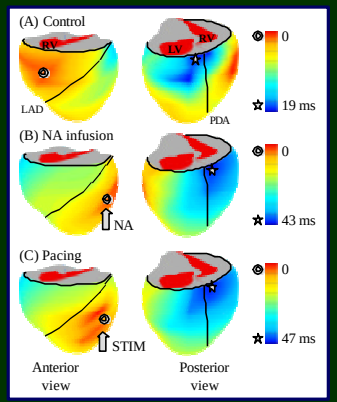

Epicardial pacing mimics events observed during the NA-induced arrhythmia

Figure 3. Epicardial activation sequences during **(A)** normal sinus rhythm and ventricular arrhythmias induced **(B)** chemically, by subepicardial NA infusion, and **(C)** electrically, using epicardial electrical stimulation (STIM). Activation maps are superimposed on a 3D mathematical model of ventricular anatomy, highlighting regions of earliest (o) and latest (*) epicardial activation. Thick lines represent the left anterior descending (LAD) and posterior descending (PDA) coronary arteries. During the ventricular arrhythmias, the location of earliest epicardial activation shifted to the infusion/stimulation site (block arrows) and the total time for spread of activation significantly increased. ABP and HR changes were also similar for the two ventricular arrhythmias and all events were fully reversible.

Ventricular activation precedes right atrial activation during the arrhythmia

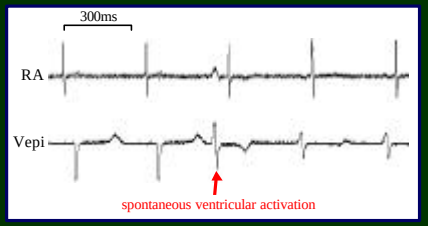

Figure 4. Right atrial (RA) versus earliest ventricular (Vepi) epicardial electropotential recordings at the onset of a NA-induced ventricular arrhythmia. Under control conditions (first two cycles) RA activation precedes Vepi, however a spontaneous ventricular activation marks the onset of the arrhythmia, after which RA activation follows Vepi activation on a one-to-one basis.

The NA-induced arrhythmia elicited significant electrical and mechanical changes

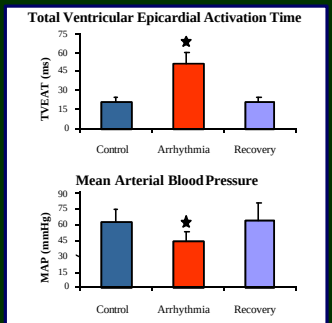

Figure 5. ★ $p < 0.005$ paired *t* test versus Control (n=14)

2D cellular network simulation

A recent model of the electrical activity in ventricular myocytes (Noble *et al.*, *Can J Cardiol* **14**:123-134, 1998) was augmented to include effects of NA on cell membrane properties in order to reconstruct the *in-vivo* experiments. To this end, the conductances of the L-type calcium current of the cell sarcolemmal membrane and the sarcoplasmic reticulum calcium-ATPase uptake current were increased five-fold. Action potential propagation was studied using a 2D sheet of 256 by 256 cells isotropically connected via linear resistors to represent the intercellular gap junctions. To simulate the spatial decrease in NA concentration due to ligand diffusion and metabolism, the calcium conductance upregulation factor was chosen to decrease according to a 2D normal distribution with a variance of 60 cell lengths so that conductance changes were negligible at a distance of 90 cell lengths from the centre. Action potentials were initiated by stimulating one edge of the sheet at a rate of 1 Hz with a twice-threshold stimulus for 2 ms. The parallel computations incorporated a variable-step fourth order Runge-Kutta numerical integration method, as described by Winslow *et al.* (*Proc R Soc Lond B* **254**:55-61, 1993).

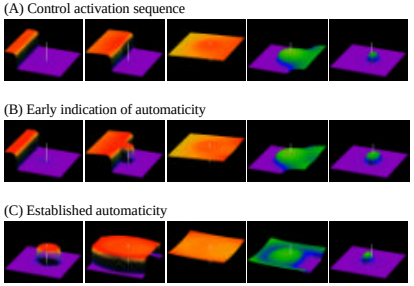

Figure 6. **(A)** The control spread of activation proceeded from left to right, where red and indigo represent regions of depolarised and repolarised tissue, respectively. The central cells were last to repolarise, since the plateau phase of their action potentials was extended due to the localised inhomogeneities in the calcium currents. **(B)** Automaticity became apparent nine cycles later, when the central region spontaneously depolarised just prior to the arrival of the control activation sequence. **(C)** A further seven cycles later, the central tissue was the dominant pacemaker and completely captured the activation sequence. The full animation may be viewed at the internet address http://www.physiol.ox.ac.uk/~dip/NEarrhythmia/2Dnetsim.mpg (MPEG movie format, 2.3 MB). *A-posteriori* analysis of the ionic currents revealed that abnormal automaticity arose from calcium overloading due to abnormal sodium-calcium activity in the central zone.

Conclusions

- 3D characterisation of the epicardial electrical events during the NA-induced ventricular arrhythmia revealed activation patterns consistent with a region of abnormal automaticity near the infusion site, which could be comprehensively mimicked by epicardial pacing.
- 2D computational reconstruction of the NA-induced arrhythmia implicated abnormal pacemaking by the sodium-calcium exchanger due to calcium overload near the infusion site.
- Interventions that reduce regional inhomogeneities in NA and intracellular calcium may prevent or terminate this type of arrhythmia.